Available online at www.sciencedirect.com
ScienceDirect
Journal of Nuclear Materials 363–365 (2007) 616–621
journal of nuclear materials
www.elsevier.com/locate/jnucmat

Edge plasma behavior in the GAMMA 10 tandem mirror based on gas puff imaging experiments with a high-speed camera

Y. Nakashima [a,*], N. Nishino [b], Y. Higashizono [a], H. Kawano [a], S. Kobayashi [c], M. Shoji [d], Y. Kubota [a], M. Yoshikawa [a], M.K. Islam [a], Y. Mishima [a], D. Mimura [a], T. Cho [a]

[a] *Plasma Research Center, University of Tsukuba, 1-1-1 Tennoudai, Tsukuba, Ibaraki 305-8577, Japan*
[b] *Graduate School of Engineering, Hiroshima University, Hiroshima 739-8527, Japan*
[c] *Institute of Advanced Energy, Kyoto University, Gokasho, Uji 611-0011, Japan*
[d] *National Institute for Fusion Science, Toki, Gifu 509-5292, Japan*

Abstract

Detailed results of edge plasma and neutral particle behavior are described in the gas puff imaging experiments performed in the GAMMA 10 tandem mirror for the first time. Visible imaging measurement by using a high-speed camera (Ultima-SE, Photron Inc.) was recently performed in the central-cell midplane of GAMMA 10. In the standard plasma discharge heated by ICRF wave, a short gas puff of hydrogen (3 ms) was carried out and the time evolution of light emission was visualized precisely. It was found that the time evolution of the emission cloud was similar to that of Hα line intensity measured nearby and was localized close to the gas puff port. Asymmetry in diffusion of the emission cloud is observed radial and axial direction of plasma column in the central-cell. This localization phenomenon of neutrals is qualitatively well explained by a fully 3-dimensional simulation using DEGAS neutral particle transport code.

PACS: 52.25.Ya; 52.40.Hf; 52.55.Jd; 52.65.Pp

Keywords: GAMMA 10; Visible imaging; Tandem mirror; Neutrals; DEGAS

1. Introduction

Measurement of edge plasmas is one of the important subjects for understanding plasma turbulence in magnetically plasma confining devices. Plasma periphery behavior also gives us useful information on plasma–wall interactions such as recycling as well as edge fluctuations. The gas puff imaging (GPI) diagnostic with high-speed camera is a powerful method for visualizing the behavior of edge plasmas as 2-dimensional (2D) images of visible light emission [1–3]. In the GAMMA 10 tandem mirror, edge plasma measurements have been performed in several location of the GAMMA

* Corresponding author. Present address: 1-1-1 Tennoudai, Tsukuba, Ibaraki 305-8577, Japan. Tel.: +81 298 53 7473; fax: +81 298 53 6202.
E-mail address: nakashma@prc.tsukuba.ac.jp (Y. Nakashima).

0022-3115/$ - see front matter © 2007 Elsevier B.V. All rights reserved.
doi:10.1016/j.jnucmat.2006.12.053

10 tandem mirror device by using Langmuir probes, calorimeter array and visible diagnostics [4–6]. Recently in GAMMA 10, visible imaging measurement by using a high-speed camera (Ultima-SE, Photron Inc.) was performed for the first time in mirror-based fusion devices [7]. In standard hot ion mode plasmas produced by ion cyclotron range of frequency (ICRF) wave, a short gas puff of hydrogen (3 ms) was carried out to illuminate the plasma periphery and the time evolution of visible light emission from the neutral cloud was investigated precisely. A short-pulse gas injection not only highlights the plasma fluctuation in the emission cloud but also provides an effective method as a tracer in itself for neutral transport analysis based on the perturbation technique. As one of the objective of this study, investigation of neutral particle behavior related to the gas puffing is focused on for the comprehensive understanding of edge plasmas besides the plasma turbulence research. In this paper, we describe the detail of 2D visible diagnostic in GPI experiments and the results are discussed mainly from the viewpoint of analyses of neutral particle transport.

2. The GAMMA 10 device and the experimental setup

Fig. 1 shows the schematic view of the GAMMA 10 tandem mirror and the experimental setup used in this study. GAMMA 10 is an effectively axisymmetrized minimum-B anchored tandem mirror with thermal barrier at both end-mirrors [8,9]. As shown in Fig. 1(a), the device consists of an axisymmetric central-mirror cell, anchor-cells with minimum-B configuration using baseball coils, and plug/barrier cells with axisymmetric mirrors. The length of the central-cell is 6 m and both ends of the central-cell are connected to the anchor-cells through the mirror throat regions. Initial plasma is produced by two plasma guns mounted on both ends and then the main plasma is built up with two ICRF waves excited in the central-cell and anchor-cells, respectively. Two gas puffers are installed for sustaining plasma at both mirror throat regions. End-loss particles along the magnetic field lines are confined by the electron-cyclotron-heating (ECH) produced plug potential in both plug/barrier cells. A number of Hα line emission detectors are installed along the machine axis (z-axis) from the central-cell midplane ($z = 0$) to the east anchor-cell ($-750\ \text{cm} < z < -300\ \text{cm}$) and two radially aligned detector arrays (x-, y-direction) are mounted near the midplane ($z = -12$ cm and -60 cm). The definition of the axes is also shown in Fig. 1(a).

Fig. 1(b) shows the cross-section view of the GAMMA 10 central-cell and the location of the high-speed camera. Hydrogen gas is puffed into the central-cell chamber from the bottom port near the midplane ($z = +12$ cm). Behavior of the plasma is monitored with the high-speed camera from the horizontal view port in the north side (right side in Fig. 1(b)). The schematic image view is shown in the right bottom of the Fig. 1(b). As shown in this view, the right side of the viewing area is obscured by the view dump which is installed for the reducing the stray light in the view area of spectrometer installed on the opposite side of the camera. A horizontal support beam interferes with the upper region of the view area. A probe head and its shaft inserted on this side also obstruct the view in the middle region. In standard condition, the high-speed camera is operated with the speed of 24.7 μs per frame (40 500 frames per second) and the frame size of 64×64 pixels.

3. Experimental results and discussion

3.1. Time behavior of plasma parameters

Fig. 2 shows an example of the time behavior of plasma parameters in GPI experiment carried out in standard hot ion mode discharges of GAMMA 10. The plasma is produced by ICRF from 50 ms to 240 ms and GPI is performed in the period of potential confinement by using ECH and NBI (180 ms–210 ms). Gas puffing from $t = 190$ ms to 193 ms increases plasma line-density by 20% and associated decrease of the diamagnetism is also observed in the central-cell. In this experiment, slightly excessive gas was puffed into the plasma in order to make sure the sufficient intensity of light emission for the high-speed camera. Consequently the intensity of Hα emission shown in Fig. 2(b) increases by 20 times larger than the base intensity near the midplane ($z = -1$ cm) and increases by 5 times at $z = -71$ cm.

3.2. Time evolution of 2-dimensional visible image

In Fig. 3, the time evolution of measured video image during and after the gas puff ($t = 192.1$ ms–$t = 195.74$ ms) is presented at intervals of 0.52 ms. In response to the gas puffing from the bottom port, 2-dimensional image of the visible emission, which

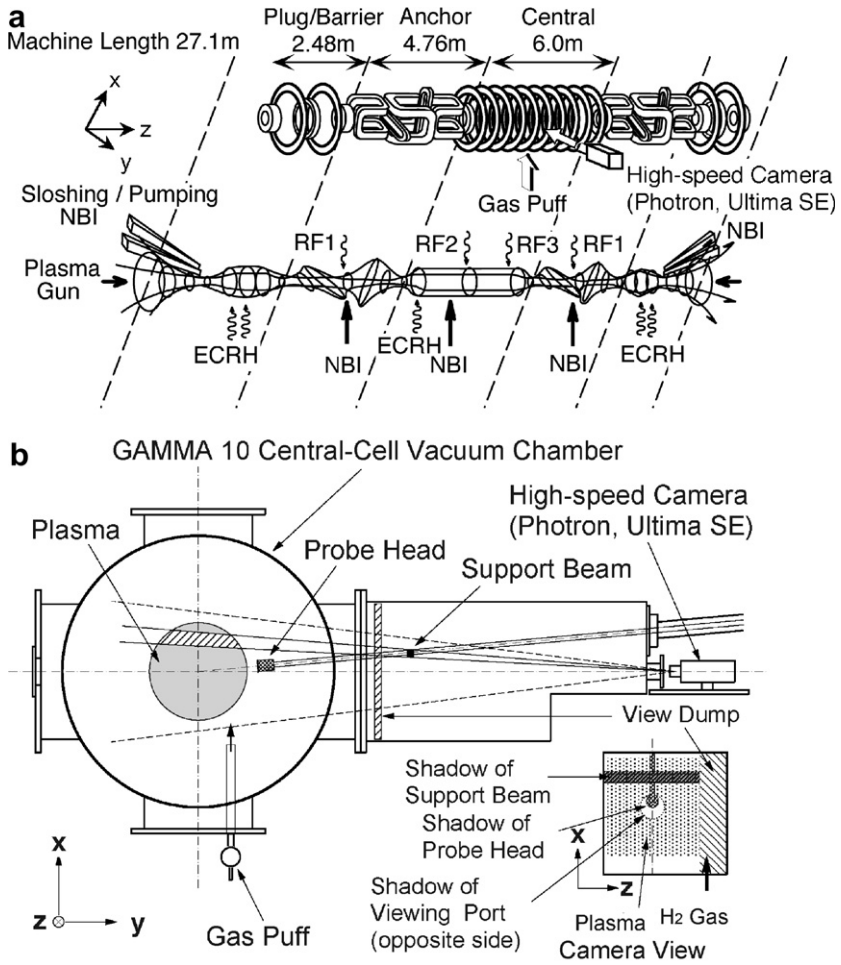

Fig. 1. The schematic view of GAMMA 10 tandem mirror and the experimental setup: (a) coil arrangement and location of high-speed camera and gas puff and (b) cross-section view of the GAMMA 10 central-cell and viewing area of the location of high-speed camera and gas puff.

shows an localization to the bottom side, is clearly confirmed. Motion of the edge plasma is also clearly observed during the illumination by gas puffing. Although it is difficult to confirm it from the sequential images shown in the figure, from Ref. [7], a vibration of plasma column was observed in this period and its FFT (fast fourier transform) and phase analyses proved that this vibration is the rotation mode with the frequency range of 4–6 kHz in the direction of electron diamagnetic drift. This observation is also consistent with the results of the visible light and Langmuir probe measurements [6]. From each image, as shown in Fig. 3, it is found that the diffusion of emission cloud along the magnetic field line (z-axis) is wider than that in radial direction (x-axis). This asymmetry of neutral penetration is explained that the mean free path of neutrals become shorter toward x-direction compared with that to z-direction, since the plasma density increases toward the plasma core region. Such localizing phenomenon is observed to be sustained in the decreasing phase of the light intensity.

3.3. Detailed behavior during GPI

Fig. 4 shows the details of the time evolution and the spatial profile of visible emission analyzed from the 2-dimensional image during gas puff. The location of sampling point from measured visible images is shown in Fig. 4(a). As shown in Fig. 4(b), Hα line emission begins to increase at 2 ms after the start of gas puff ($t = 190$ ms) and reaches its peak ~1 ms after the termination of gas puff. This delay is considered to be due to the conductance of the guide

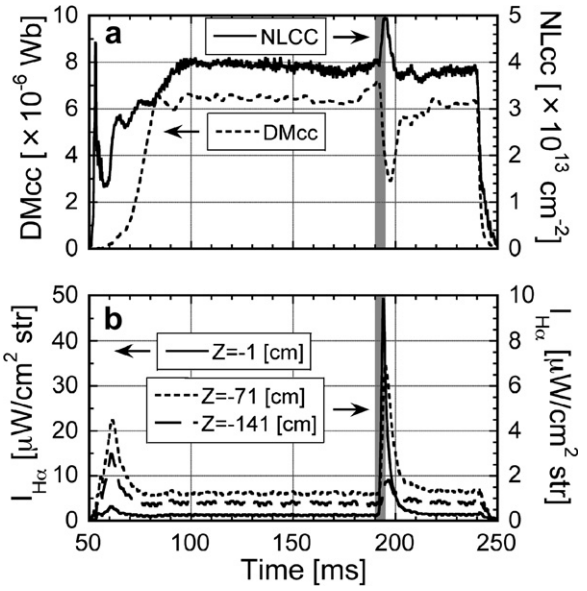

Fig. 2. Time behavior of plasma parameters in the present experiment: (a) electron line-density (NLcc) and diamagnetism (DMcc) measured in the central-cell and (b) Hα line intensity signal measured at three different positions in the central-cell.

pipe attached to the exit of the piezo valve. On the other hand, plasma line-density begins to rise with the increase of the Hα intensity and keeps constant in 2 ms after the peak of Hα intensity, then slowly decreases. Fig. 4(d) shows the time behavior of the image intensity measured at different positions (45, 33), (45, 38), (45, 50) along the direction of gas injection (x-direction). The image intensity in each pixel position shows exactly similar time dependence to Hα line intensity shown in Fig. 4(b), which implies that visible emission from the plasma is mainly ascribed to Hα line emission. Fig. 4(c) shows the time evolution of intensity spatial profile in the vertical axis (x-pixel) at $z = 45$ pixel position. During the increasing phase ($192\ \text{ms} < t < 194\ \text{ms}$), each peak position stays at a fixed place ($x = 50$ pixel) and then it moves slightly upward after termination of gas puff. At the present, it is not identified that the above movement indicates diffusion into the plasma core or streaming upward along the plasma periphery region.

3.4. Monte-Carlo simulation of GPI

In order to quantitatively investigate the above characteristics in the localization of the emission cloud shown in Fig. 4, Monte-Carlo simulation was carried out in the central-cell by using DEGAS neutral transport code [10,11]. In GAMMA 10, neutral transport analysis has been performed based on Hα emission diagnostics and Monte-Carlo simulation [12–15]. Fig. 5(a) shows the schematic view of the plasma mesh model used in the simulation. A fully 3-dimension mesh model of DEGAS ver.63 code has been developed for this purpose [16]. A particle source is defined at the position of gas puff exit as a secondary wall. In Fig. 5(b), a cross-section view of Hα line emissivity is presented in the x–y

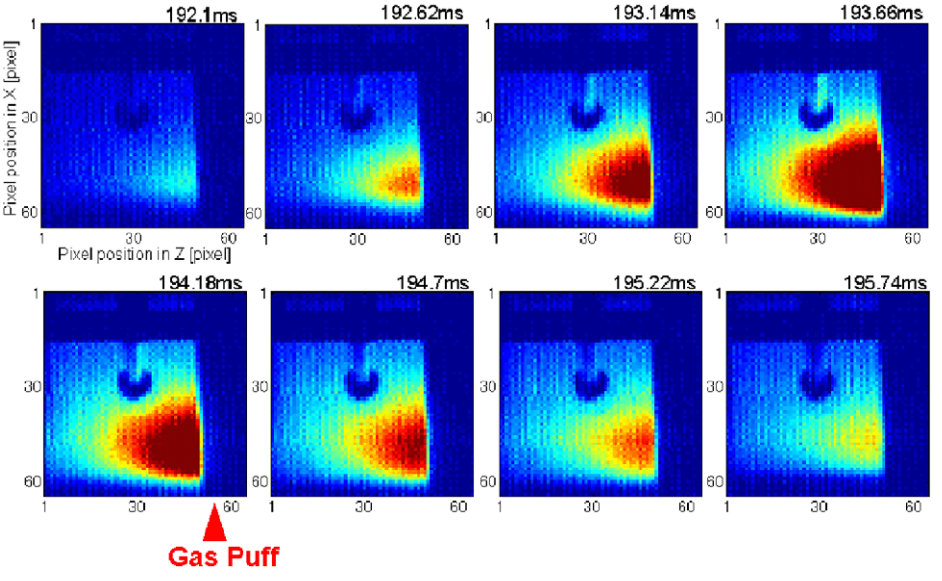

Fig. 3. Time evolution of 2-dimensional visible images during and after gas puff.

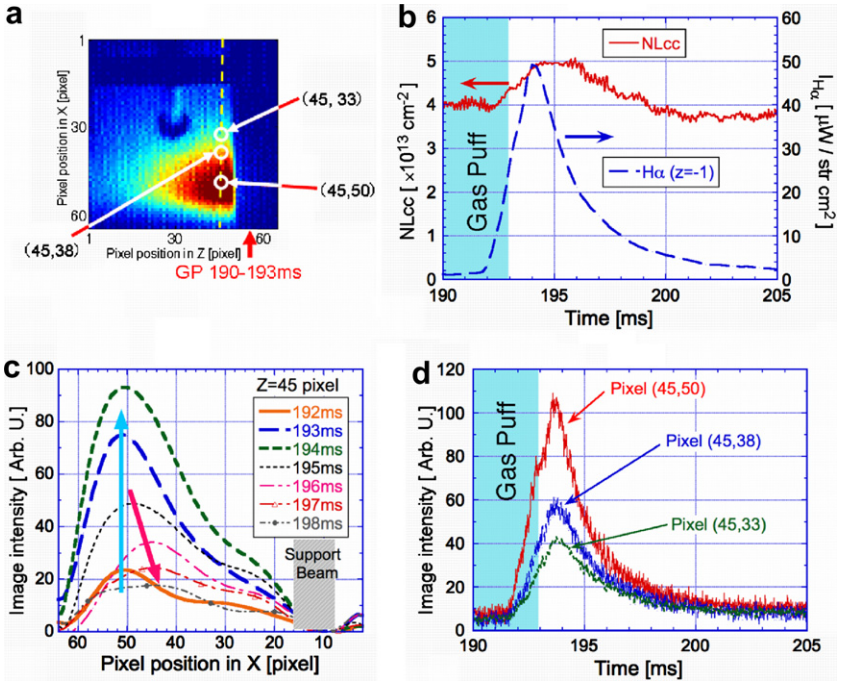

Fig. 4. Detailed time evolution and spatial profile of visible emission analyzed from the 2-dimensional image: (a) locations of the sampling pixel in the 2D image, (b) time behavior of electron line density NLcc and the Hα line intensity at $z = -1$ cm, (c) spatial profile of the image intensity and (d) time evolution of the image intensity on three different pixels.

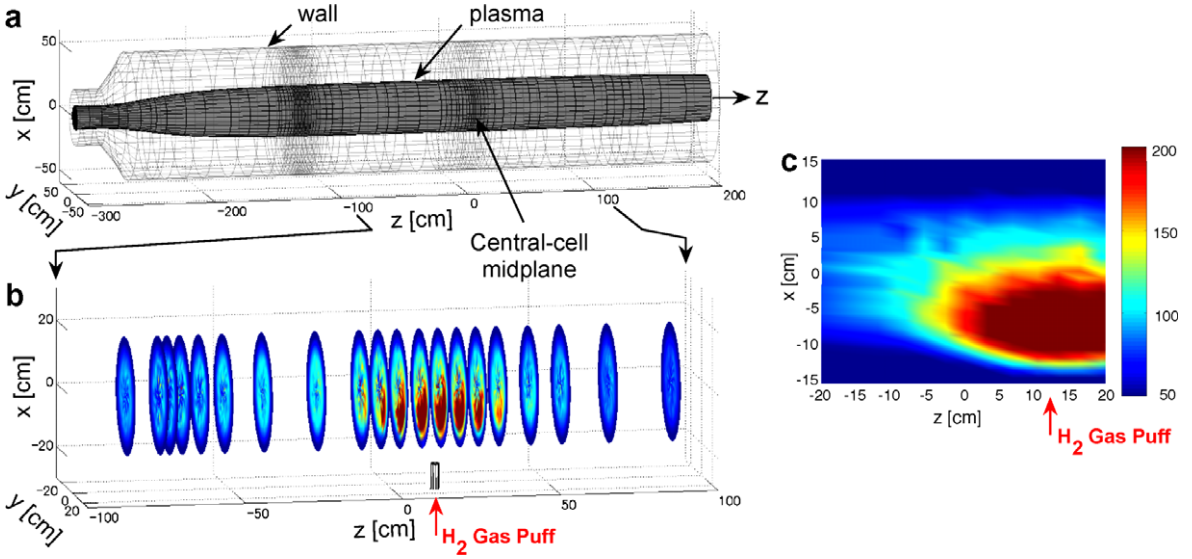

Fig. 5. Result of Monte-Carlo simulation in GPI experiment: (a) mesh model of the GAMMA 10 central-cell used in the simulation, (b) cross-section view of Hα line emissivity at each axial position (-100 cm $< z <$ 100 cm) and (c) Hα line intensity simulated in the camera view.

plane at each axial position (-100 cm $< z <$ 100 cm). By integrating the emissivity along the sight line of the camera view, 2-dimensional image of the Hα intensity is predicted as shown in Fig. 5(c). The simulation result agrees well with the experimental one. Particularly on observed

asymmetry shown in Fig. 4(a), the simulation adequately reproduces the observation result. In this simulation dissociative excitation processes of hydrogen molecules are considered in the light emission as well as neutral transport [12]. The contribution of hydrogen molecules to the total emission is estimated to 20% just under the gas-injection position due to the low density of the plasma ($n_e \sim$ few $\times 10^{12}$ cm^{-3}), since the Franck–Condon atoms deeply penetrate into the plasma core region and the resultant emission intensity and its area become dominant. From the above results, GPI exhibits powerful ability not only for the edge plasma diagnostics but also for quantitative analysis on localization and complicated behavior of neutrals.

4. Summary

Precise measurements of 2-dimensional image have been performed successfully in the first experiment of the gas puff imaging with a high-speed camera in the central-cell of the GAMMA 10 tandem mirror. From the 2-dimensional image analyses of the light emission, it was confirmed that there is a similarity in the time dependence to the Hα intensity measured nearby. It was found that a significant asymmetry in the neutral diffusion between transverse direction of plasma column and direction along the machine axis. Localization of the emission cloud was recognized near the gas puff and the result of Monte-Carlo simulation reproduced the experiment very well. These results establish the effectiveness of GPI in the mirror machine and GPI provides a powerful analysis method for clarification of complex behavior in 3-dimensional neutral transport which is useful for the other plasma confinement devices.

Acknowledgements

This study was supported by the bilateral collaboration research program in the University of Tsukuba, Hiroshima University, Kyoto University and NIFS. The authors would like to acknowledge the members of the GAMMA 10 group, University of Tsukuba for their help in the experiments.

References

[1] S.J. Zweben et al., Phys. Plasmas 9 (2002) 1981.
[2] R.J. Maqueda et al., Rev. Sci. Instrum. 74 (2003) 2020.
[3] J.L. Terry et al., J. Nucl. Mater. 290–293 (2001) 757.
[4] Y. Nakashima et al., J. Plasma Fusion Res. SERIES 5 (2002) 428.
[5] Y. Nakashima et al., Rev. Sci. Instrum. 75 (No. 10 Part II) (2004) 4308.
[6] H. Higaki et al., Rev. Sci. Instrum. 75 (No. 10 Part II) (2004) 4085.
[7] N. Nishino, Y. Nakashima, et al., Plasma Fusion Res. 1 (2006) 035.
[8] M. Inutake et al., Phys. Rev. Lett. 55 (1985) 939.
[9] T. Cho et al., Trans. Fusion Technol. 47 (No.1T) (2005) 9.
[10] D. Heifetz, D. Post, M. Petravic, et al., J. Comput. Phys. 46 (1982) 309.
[11] D.P. Stotler et al., Phys. Plasmas 3 (1996) 4084.
[12] Y. Nakashima et al., J. Nucl. Mater. 196–198 (1992) 493.
[13] Y. Nakashima et al., J. Nucl. Mater. 241–243 (1997) 1011.
[14] Y. Nakashima et al., J. Plasma Fusion Res. SEREIS 6 (2004) 546.
[15] S. Kobayashi et al., J. Nucl. Mater. 266–269 (1999) 566.
[16] Y. Nakashima et al., J. Nucl. Mater. 337&339 (2005) 466.